Chapter 13

Retrograde Axonal Transport of Neurotrophins in Basal Forebrain Cholinergic Neurons

Arman Shekari and Margaret Fahnestock

Abstract

Axonal transport is key for the survival and function of all neurons. This process is especially important in basal forebrain cholinergic neurons due to their extremely long and diffuse axonal projections. These neurons are critical for learning and memory and degenerate rapidly in age-related neurodegenerative disorders like Alzheimer's and Parkinson's disease. The vulnerability of these neurons to age-related neurodegeneration may be partially attributed to their reliance on retrograde axonal transport for neurotrophic support. Unfortunately, little is known about the molecular biology underlying the retrograde transport dynamics of these neurons due to the difficulty associated with their maintenance in vitro. Here, we outline a protocol for culturing primary rodent basal forebrain cholinergic neurons in microfluidic chambers, devices designed specifically for the study of axonal transport in vitro. We outline protocols for labeling neurotrophins and tracking neurotrophin transport in these neurons. Our protocols can also be used to study axonal transport in other types of primary neurons such as cortical and hippocampal neurons.

Key words Neurotrophins, Cholinergic, Microfluidic chambers, Aging, BDNF, NGF, proNGF, Axonal transport, Basal forebrain, Retrograde

1 Introduction

Intracellular trafficking is critical for the survival and proper function of all neurons due to their extreme structural and biochemical polarity. Neurons orchestrate the bidirectional transport of a wide variety of cellular cargo, from proteins and RNA to entire organelles, along their lengthy axonal projections in a tightly regulated manner via a process termed axonal transport [1]. Axonal transport occurs along microtubules, cytoskeletal elements composed of polarized tubulin polymers that span the entirety of the axon [2]. These polymers are organized in parallel radial arrays, forming unipolar filaments with plus ends proximal to the axon tip and minus ends proximal to the cell body [2, 3]. The transport of cargo toward the axon tip is referred to as anterograde or "plus-

Alessio Vagnoni (ed.), *Axonal Transport: Methods and Protocols*,
Methods in Molecular Biology, vol. 2431, https://doi.org/10.1007/978-1-0716-1990-2_13,

end directed" while transport toward the cell body is referred to as retrograde or "minus-end directed."

Anterograde and retrograde transport occur via the procession of two classes of ATP-dependent molecular motors along microtubules: kinesin and dynein. Kinesin family motor proteins are responsible for carrying out anterograde transport, while the cytoplasmic dynein motor protein is responsible for carrying out retrograde transport [2, 4]. Both kinesin family and dynein motors are large and complex proteins consisting of multiple polypeptide chains classified as either heavy, light, or intermediate chains, depending on their molecular weight [5]. The association of these chains via their N-terminal tail domains creates binding domains for cargo adapter proteins [2]. A wide variety of adapter proteins exist and facilitate critical functions of both kinesin family and dynein motors, including the binding of cargo to the motors themselves and the binding of motors to microtubule tracks [2, 6–9].

While the motor proteins underlying retrograde and anterograde transport share some similarities, they, like the transport processes they govern, are distinct from one another. This chapter will focus largely on retrograde axonal transport, specifically within the basal forebrain, a brain area where deficits in retrograde transport have been heavily implicated in the development of age-related neurodegenerative disorders [10, 11].

The basal forebrain is located at the ventral rostrocaudal extent of the brain and consists of multiple structures including the diagonal band of Broca, nucleus basalis of Meynert, and the medial septal nucleus [12, 13]. Most neurons within these structures produce the neurotransmitter acetylcholine, making the basal forebrain the major cholinergic output of the central nervous system (CNS). Basal forebrain projections are extremely lengthy and diffuse, projecting upward and terminating widely throughout the hippocampus and neocortex [12, 13]. These projections are critical for learning, memory, and attention, making the basal forebrain a vital cognitive center [13].

The degeneration of ascending basal forebrain cholinergic projections occurs both in normal aging and with increased severity in age-related neurodegenerative disorders like Alzheimer's and Parkinson's disease [14–16]. Loss of cholinergic innervation correlates strongly with cognitive decline and is considered a hallmark of Alzheimer's disease (AD) [13, 15, 17, 18]. Basal forebrain cholinergic neurons (BFCNs) demonstrate a striking selective vulnerability in AD, as they are among the first neurons in the brain to degenerate in the disorder [15, 18–22]. This vulnerability results in up to 95% of BFCNs degenerating by the end stages of AD [23, 24].

One factor that may explain the selective vulnerability of BFCNs to age-related neurodegenerative disorders is their inability

to produce a family of growth factors termed neurotrophins. Neurotrophins are a family of extracellular signaling proteins that are critical for neuronal development, survival, and plasticity [25]. BFCNs are dependent upon the neurotrophins nerve growth factor (NGF) and brain derived neurotrophic factor (BDNF) for their survival and function [26–32]. NGF and BDNF, like all neurotrophins, are initially synthesized as proproteins that can be processed to their mature forms [33]. However, proneurotrophins are capable of facilitating intracellular signaling independently of their mature counterparts [34–37]. Additionally, while pro and mature BDNF and proNGF are detectable in the mammalian CNS, mature NGF is not, further highlighting the importance of studying proneurotrophins in the context of CNS neurons like BFCNs [38–40].

BFCNs are reliant on their synaptic targets in the hippocampus and cortex for their supply of BDNF and proNGF [41–43]. Upon release, these neurotrophins bind to either tropomyosin-related kinase (Trk) or $p75^{NTR}$ receptors at BFCN axon terminals and are retrogradely transported to BFCN cell bodies [10, 11, 25, 41, 44, 45]. In AD and in animal models of AD, NGF-immunoreactive material accumulates in BFCN target areas and is decreased in the basal forebrain itself, suggesting impaired retrograde neurotrophin axonal transport [46, 47]. Additionally, both BDNF and proNGF retrograde transport are reduced in aged BFCNs, further implicating dysfunctional retrograde transport in the selective vulnerability of these neurons to age-related neurodegeneration [10]. Unfortunately, the mechanisms underlying these observed transport deficits are currently unknown. In fact, very little is known about the mechanisms governing retrograde neurotrophin transport in this highly vulnerable neuron population.

The mechanistic study of retrograde neurotrophin transport is complicated by the diffuse and highly arborized projections primary neurons develop in vitro. Organizing and separating neuronal cell bodies and axon terminals facilitates the accurate assessment and quantification of axonal transport in vitro. Recently, microfluidic chambers have been developed to achieve this organization and to advance the direction-specific assay of axonal transport in CNS neurons [48, 49]. These chambers contain microgrooves that are connected to a main channel that houses neuronal cell bodies. Axons grow through these microgrooves and emerge into another channel that maintains fluidic isolation from the channel that houses the cell bodies, permitting the independent manipulation of neuronal cell bodies and axons. This fluidic isolation allows neurotrophins to be administered exclusively to the axon terminals of neurons. The microgrooves also linearize axons and enable anterograde and retrograde transport to be accurately quantified. While BFCNs seem like ideal candidates for study using

microfluidic chambers due to their unique reliance on retrograde transport, they are difficult to maintain in vitro.

Here we describe a protocol for the culture and maintenance of embryonic rodent BFCNs in microfluidic culture, as well as a protocol for the tracking of retrograde transport of biotinylated neurotrophins conjugated to streptavidin-labeled quantum dot fluorophores. We provide a protocol for the purification of biotinylated proNGF from the medium of human embryonic kidney (HEK) cells transfected with a plasmid coding for Avi-tagged, cleavage-resistant proNGF [10, 50]. We also provide a protocol for the immunocytochemical analysis of these neurons to validate cholinergic phenotype. These protocols may be used in conjunction with other primary neuron types such as cortical neurons, however with some minor modifications that are mentioned below.

2 Materials

2.1 Preparation of Microfluidic Chambers

1. XC450 Microfluidic devices (Xona Microfluidics, Research Triangle Park, NC, USA).
2. Precoat ethanol solution (Xona Microfluidics, included with XC450 devices).
3. Humidity-controlled ChipTrays™ (Recommended only, *see* **Note 1**) (Xona Microfluidics).
4. 1× phosphate buffered saline (PBS): 137 mM NaCl, 2.7 mM KCl, 10 mM Na_2HPO_4, and 1.8 mM KH_2PO_4. Adjust solution to pH 7.4.
5. 0.01% sterile-filtered poly-L-lysine (PLL) solution.

2.2 Dissection and Processing of Basal Forebrain Tissue

1. Dissection tools suitable for embryonic murine dissection (fine-tip Dumont forceps and scissors, tweezers, petri dishes).
2. Dissection microscope.
3. Clinical centrifuge capable of reaching 250 × *g*.
4. Hemocytometer.
5. 100× penicillin–streptomycin (P/S) (10,000 units/mL of penicillin and 10,000 μg/mL of streptomycin).
6. 1× Hanks's Balanced Salt Solution (HBSS): Dilute 10× HBSS stock solution using sterile double-distilled water, add 1% P/S and pH to 7.4 before sterile filtering.
7. Fine fire-polished glass Pasteur Pipettes: Expose the tip of a glass Pasteur pipette to the flame of a Bunsen burner for a few seconds while rotating the base of the pipette. Repeat until the tip has become smooth and the opening has shrunk to about 1 mm in diameter (*see* **Note 2**). Autoclave and keep sterile before use.

8. DNase I solution (1 mg/mL).
9. 10× trypsin–EDTA solution.
10. BFCN Plating Medium: Neurobasal medium, 1% P/S, 2% B27 serum-free supplement, 1% GlutaMAX, 10% fetal bovine serum (FBS), 50 ng/mL recombinant murine BDNF (Peprotech, Rocky Hill, NJ, USA), 50 ng/mL recombinant human β-NGF (Peprotech).

2.3 Plating and Maintenance of BFCNs in Microfluidic Chambers

1. BFCN Plating Medium: Neurobasal medium, 1% P/S, 2% B27 serum-free supplement. 1% GlutaMAX, 10% fetal bovine serum (FBS), 50 ng/mL recombinant murine BDNF, 50 ng/mL recombinant human β-NGF.
2. BFCN Maintenance Medium: Neurobasal medium, 1% P/S, 2% B27 serum-free supplement, 1% GlutaMAX, 50 ng/mL recombinant murine BDNF, 50 ng/mL recombinant human β-NGF (*see* **Note 3**).

2.4 Immunocytochemical Staining of BFCNs in Microfluidic Chambers

1. Widefield or confocal microscope capable of fluorescence microscopy.
2. 4% paraformaldehyde (PFA) sterile solution: Dilute 1 g of PFA powder per 15 mL of sterile water. Water should be heated to 60 °C before addition of PFA. Add 1 N NaOH until powder has fully dissolved, then add 10 mL of 3× PBS for every 15 mL of water. Adjust the pH of the solution to 7.2 and sterile filter before use.
3. 10% Triton X-100 Solution.
4. PBS-A: 0.01% Triton X-100 diluted in 1× PBS.
5. PBS-B: Dissolve 300 mg bovine serum albumin in ~8 mL of 1× PBS and add 500μL of FBS. Bring the solution to a final volume of 10 mL, and sterile filter before use.
6. Primary antibodies: Any primary antibody compatible with immunocytochemistry can be used. To confirm cholinergic phenotype, vesicular acetylcholine transporter (VAChT, Santa Cruz Biotechnology, Dallas, TX, USA) antibodies can be used. TrkA antibodies (Alomone Labs, Jerusalem BioPark, Israel) can also be used to confirm cholinergic phenotype, as BFCNs express TrkA [51, 52].
7. Secondary antibodies: Any secondary antibodies compatible with immunocytochemistry can be used. Our lab uses Alexa-Fluor antibodies.
8. DAPI nuclear counterstain.
9. Silicone immersion oil (Ibidi, Fitchburg, WI, USA) (*see* **Note 4**).

2.5 Purification of Biotinylated proNGF

1. HEK293-FT cells (ATCC, Manassas, VA, USA).
2. Centrifuge capable of reaching speeds of 300 × *g*.
3. 10 kDa centrifugal concentrators.
4. Cold room or large refrigerator.
5. HEK Plating Medium: Dulbecco's Modified Eagle Medium (DMEM), 10% FBS, 1% GlutaMAX, 1% P/S, 1% sodium pyruvate, 1% nonessential amino acids.
6. HEK Transfection Medium: Dulbecco's Modified Eagle Medium (DMEM), 1% GlutaMAX, 1% P/S, 1% sodium pyruvate, 1% nonessential amino acids, 1 mg/mL d-biotin.
7. Turbofect™ transfection reagent (ThermoFisher Scientific).
8. Nickel nitrilotriacetic acid (Ni-NTA) resin.
9. Reusable nickel purification columns.
10. proNGF-R-1G-Avi-His and Bir-A biotin ligase pcDNA-3.1 plasmids [10, 50] (Bir-A biotin ligase plasmid also available from Addgene, Watertown, MA, USA).
11. Ni-NTA wash buffer: 1× PBS, 20 mM imidazole, 1 mM phenylmethylsulfonyl fluoride (PMSF). Adjust to a final pH of 8.0.
12. Ni-NTA elution buffer (50 mL): 1× PBS, 300 mM imidazole, phosSTOP, and ULTRA tablets (Roche, Basel, Switzerland). Adjusted to a final pH of 8.0.

2.6 Tracking and Analysis of Neurotrophin Axonal Transport

1. Widefield or confocal microscope equipped with an on-stage incubator capable of maintaining 37 °C, 5% CO_2 and capable of fluorescence microscopy.
2. Quantum dot (Qdot) 625-streptavidin conjugate (ThermoFisher Scientific) (*see* **Note 5**).
3. Qdot625 or Texas Red fluorescence filter cube set (*see* **Note 6**).
4. DAPI and Cy5 fluorescence filter cube set.
5. Biotinylated neurotrophins (Alomone or via Ni-NTA chromatography).
6. TubulinTracker™ Deep Red (ThermoFisher Scientific), optional (*see* **Note 7**).
7. Axonal Imaging Medium: Neurobasal medium minus phenol red, 1× P/S, 1× B27 serum-free supplement, 1× GlutaMAX.
8. Somal Imaging Medium: Neurobasal medium minus phenol red, 1% P/S, 2% B27 serum-free supplement, 1% GlutaMAX, 50 ng/mL recombinant BDNF, 50 ng/mL recombinant β-NGF.
9. NucBlue™ LiveReadyProbes™ Hoechst nuclear counterstain (ThermoFisher Scientific).

10. ImageJ 1.53c equipped with the "ImageScience" plugin set (included with ImageJ) and the KymoToolBox plugin (available from: https://github.com/fabricecordelieres/IJ-Plugin_KymoToolBox).

3 Methods

3.1 Preparation of Microfluidic Chambers (To Be Done 24 h Before Dissection)

XC450 devices must be sterilized using the included precoat solution before use. The devices must also be coated with an adhesion substrate, in this case poly-L-lysine (PLL), to improve the adherence of primary neurons to the channels of the device. Working with microfluidic chambers requires a great deal of patience and care. The fluidic isolation and neuronal organization these devices provide is only possible if the devices are handled optimally, which we outline below (Figs. 1 and 2).

1. Within a biosafety cabinet, add 100 μL of precoat solution to the top left well of each chamber (Fig. 1) and let stand for 1 min (*see* **Note 8**).
2. Add 100 μL of precoat solution to the bottom left well of each chamber and let stand for 5 min.
3. Add 100 μL of precoat solution to the top right well of each chamber and let stand for 1 min.
4. Add 100 μL of precoat solution to the bottom right well of each chamber and let stand for 5 min.
5. Aspirate the precoat solution from every well, making sure to leave ~20 μL of residual solution within each well, and immediately add 150 μL of PBS to the top left well of each chamber. Let stand for 1 min (*see* **Notes 9** and **10**).
6. Repeat **steps 2–5** with 150 μL of PBS (Fig. 1).
7. Add 150 μL of PBS to both top wells of the device. Immediately repeat for both bottom wells (Fig. 2).
8. Aspirate the PBS solution from all wells and then repeat steps 1–4 using 120 μL of 0.01% PLL solution (warmed to 37 °C) (Fig. 1).
9. Place chambers in a 37 °C, 5% CO_2 incubator for 24 h.
10. Inspect all chambers to ensure no bubbles have formed within the main channels (*see* **Note 11**).
11. Aspirate the PLL from all wells and repeat **steps 1–4** with 150 μL of PBS.
12. Aspirate the PBS from all wells and add 150 μL of plating medium that has been warmed to 37 °C to both top wells of the device (Fig. 2). Immediately repeat for both bottom wells.
13. Store chambers in a 37 °C, 5% CO_2 incubator until plating.

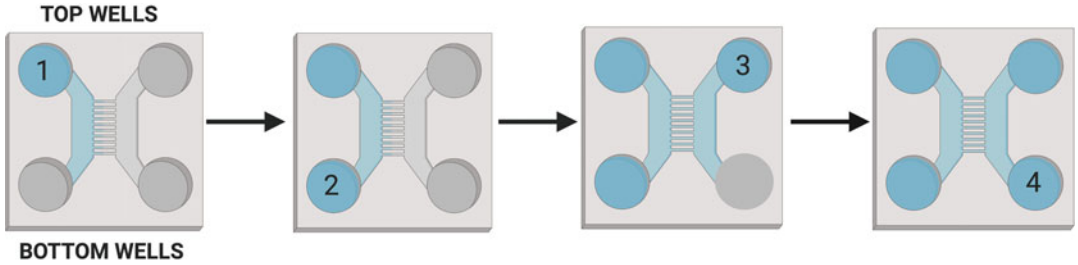

Fig. 1 Microfluidic device schematic depicting the well order to be followed during device preparation

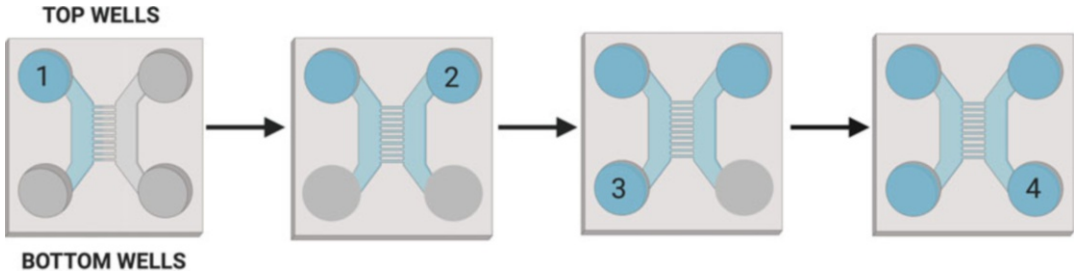

Fig. 2 Microfluidic device schematic depicting the well order to be followed during media changes and washes. This well order is also used once during device preparation for the second PBS incubation

3.2 Dissection and Processing of Embryonic Basal Forebrain Tissue (Fig. 3)

The basal forebrain is relatively small compared to commonly dissected neural structures like the cortex and hippocampus. Thankfully, its structure is very distinct and can be easily distinguished from neighboring brain areas. The small working volumes afforded by microfluidic culture allow many chambers to be prepared using a minimal amount of tissue.

The following protocol can also be used for preparing cortical and hippocampal neuronal cultures. These neurons are far more robust in culture and can be plated at higher densities than basal forebrain (within the 10^5 cells/mL range). The plating medium for cortical and hippocampal neurons does not need to contain any neurotrophins.

1. Sacrifice a pregnant rat or mouse at embryonic day (E)18 using CO_2 euthanasia or cervical dislocation and remove all embryos (*see* **Note 12**). Place embryos on ice.
2. Remove embryos from the embryonic sac using fine Dumont forceps, and separate the head from the body using a small pair of scissors. Place the head in a petri dish containing a small amount of cold HBSS solution and remove the brain from the skull using fine Dumont forceps.
3. Place the brain in a separate petri dish containing a small amount of HBSS. Under a dissection microscope, remove the meninges from the brain using fine Dumont forceps.

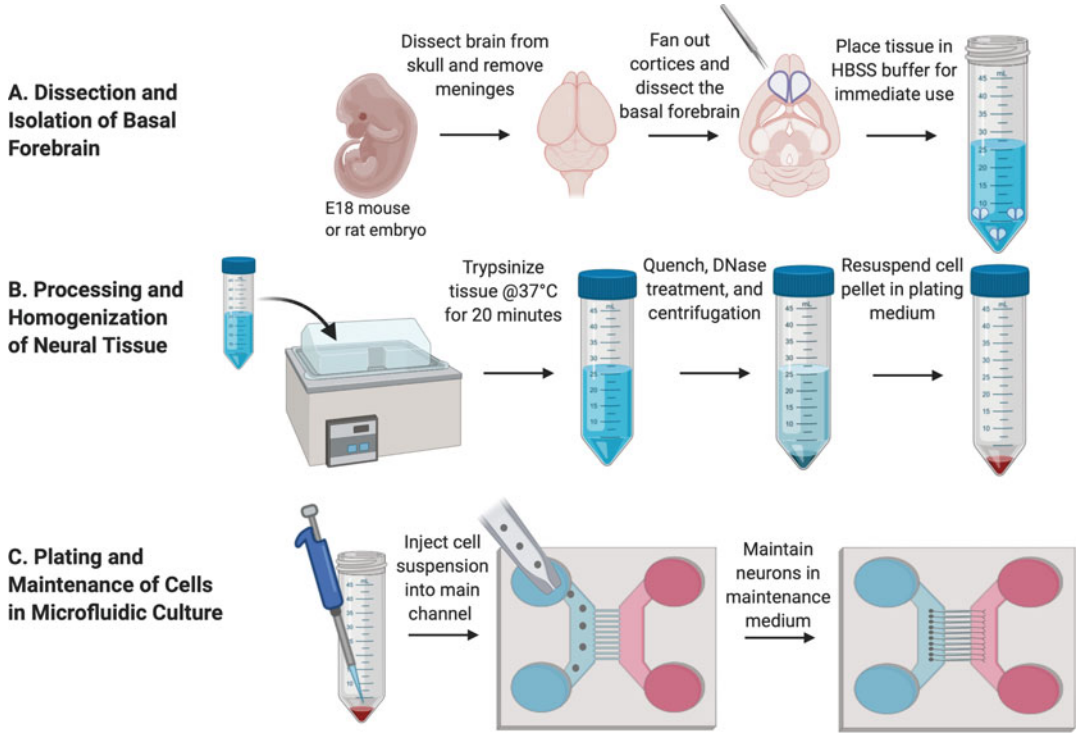

Fig. 3 Graphical depiction of the dissection and processing procedure outlined in Subheading 3.2

4. Remove the olfactory bulbs using a small pair of scissors. Place two medial cuts at the front of each cortical lobe. Fan out each lobe to expose the basal forebrain (*see* **Note 13**). Remove the basal forebrain from the brain using a pair of small scissors. Aspirate the tissue into a tube filled with a small amount of cold HBSS, and place on ice.
5. Repeat **steps 2–4** for each embryo (*see* **Note 14**).
6. In a biosafety cabinet, aspirate as much HBSS solution as possible from the collection tube without disturbing the tissue. Add 1 mL of fresh, cold HBSS to the tube. Repeat 5 times to wash.
7. Aspirate as much HBSS solution from the collection tube as possible without disturbing the tissue. Add 450 μL of fresh, cold HBSS to the tube. Immediately add 50 μL of 10× trypsin-EDTA to the tub and incubate in a 37 °C water bath for 20 min, gently agitating the tube every 5 min.
8. Add 50 μL of 10× DNase I to the collection tube. Triturate the tissue using a fire-polished glass Pasteur pipette until the solution becomes cloudy and no visible chunks of tissue remain. Add 1 mL of plating medium warmed to 37 °C to quench the trypsin.

9. Centrifuge the solution at 250 × *g* for 4 min and remove the supernatant. Resuspend the cell pellet using warm plating medium to a final density of 1×10^6 cells/mL using a hemocytometer. Repeatedly triturate this cell mixture to ensure homogeneity.

3.3 Plating and Maintenance of BFCNs in Microfluidic Chambers

BFCNs are difficult to maintain in culture and require consistent medium changes using neurotrophin-rich medium. These neurons must be plated at high densities (in the range of 10^6 cells/mL) to be viable in microfluidic culture. BFCNs produce axonal projections in vitro that cross the microgrooves in a matter of days if properly maintained (Fig. 4).

Cortical and hippocampal neurons can also be maintained using this protocol. However, like the plating medium, the maintenance medium used for these neurons does not need to contain any neurotrophins.

1. In a biosafety cabinet, aspirate the plating medium from all wells (*see* **Note 9**).
2. Inject 10 μL of the previously prepared cell solution into the top left well of the chamber by placing the tip of the pipette directly adjacent to the opening of the main channel to ensure the cell solution flows from the well into the main channel (*see* **Note 15**). Repeat for the bottom left well and place the chambers in a 37 °C, 5% CO_2 incubator for 5 min to allow neuronal adherence to the substratum.
3. Add 150 μL of plating medium to both top wells. Immediately repeat for both bottom wells. Incubate the chambers at 37 °C, 5% CO_2 for 24 h.
4. Replace the plating medium with maintenance medium after 24 h (Fig. 2). Repeat every 48–72 h (*see* **Notes 9** and **10**). Axonal projections usually take 5–7 days to cross the microgrooves (Fig. 3). Basal forebrain neurons maintain transport for 2 weeks [10] (*see* **Note 16**).

3.4 Immunocytochemical Staining of BFCNs in Microfluidic Chambers

Immunostaining neurons cultured in microfluidic chambers requires many incubations and washes. This is mainly due to the restrictive opening joining the wells of the device to the main channels. High quality images comparable to those obtained using cells cultured in standard well plates on glass coverslips can be obtained from microfluidic chambers using this protocol (Fig. 5).

1. In a biosafety cabinet, perform a PBS wash by replacing the maintenance medium in all wells with 150 μL of PBS. Immediately replace the PBS with a 4% PFA solution (*see* **Notes 9** and **10**). Incubate at room temperature for 30 min in a light-proof

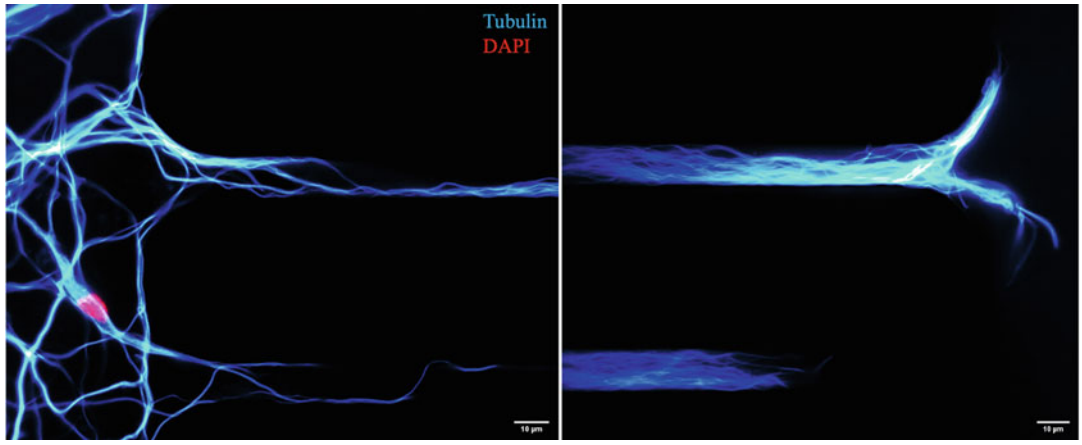

Fig. 4 Basal forebrain cholinergic neurons (BFCNs) stained for tubulin (cyan) and DAPI (red) at day in vitro (DIV) 5. The left panel depicts BFCN cell bodies extending their axons into the microgrooves. The right panel depicts BFCN axons extending across the entire length of the 450 μM microgroove barrier and beginning to enter the axonal main channel

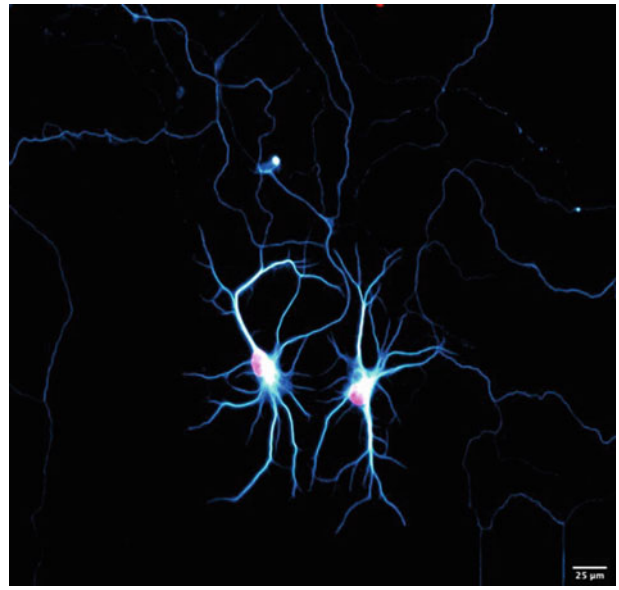

Fig. 5 Basal forebrain cholinergic neurons (BFCNs) cultured in microfluidic chambers stained for tubulin (cyan) and DAPI (red) at day in vitro (DIV) 7 following the immunocytochemical staining protocol outlined in Subheading 3.4

box. The chambers must be protected from light during all subsequent incubations.

2. Perform a PBS wash with 150 μL of PBS and then immediately add 150 μL of PBS-A to all wells (*see* **Notes 9** and **10**). Incubate at room temperature for 30 min.

3. Replace the PBS-A solution with 150 μL of PBS-B per well (*see* **Notes 9** and **10**). Incubate at room temperature for 30 min. During this time, prepare the primary antibody solution using PBS-B as the diluent.
4. Replace the PBS-B solution with 150 μL of the primary antibody solution per well (*see* **Notes 9** and **10**). Incubate at 4 °C overnight.
5. Perform 3 washes using 150 μL of PBS-B per well (*see* **Notes 9** and **10**). Incubate at room temperature for 10 min in between each wash. During the last wash, prepare the secondary antibody solution using PSB-B as the diluent.
6. Replace the PBS-B solution with 150 μL of the secondary antibody solution per well (*see* **Notes 9** and **10**). Incubate at room temperature for 2 h. During this time, prepare a DAPI nuclear counterstain using PBS as the diluent.
7. Aspirate the secondary antibody solution from all wells and add 150 μL of the DAPI counterstain solution to the top left well, followed by 150 μL of PBS to the top right well. Repeat this for the bottom two wells and incubate at room temperature for 10 min.
8. Perform two 150 μL PBS washes. Incubate at room temperature and wait 5 min between each wash. Perform two additional 150 μL PBS washes in immediate succession (*see* **Notes 9** and **10**).
9. Image the cells using either wide field or confocal fluorescence microscopy (*see* **Note 17**).

3.5 Purification of Biotinylated proNGF

Our lab uses a slightly modified version of the protocol outlined in Sung et al. (2011) to obtain monobiotinylated proNGF from transfected HEK cell medium [50]. HEK cells are grown in a biotin-containing transfection medium and are cotransfected with the biotin-ligase coding construct BirA and our custom proNGF construct. Biotinylation of proNGF occurs due to the inclusion of a biotin-accepting AviTag™ region within our construct. This process can be skipped when studying BDNF, proBDNF, and NGF, as biotinylated versions of these neurotrophins are available commercially (Alomone). Due to the lack of mature NGF in the CNS, we recommend the use of proNGF over mature NGF when studying transport in CNS neurons [10, 38].

1. Plate HEK293 cells at an initial density of $1.5x10^6$ cells/ml. Grow to ~50% confluence in 30 ml growth medium in a 30 cm petri dish.
2. In a biosafety cabinet, replace the growth medium with transfection medium and incubate cells for 72 h at 37 °C, 5% CO_2.

3. Dilute 20 μg of proNGF-R-1G-Avi-His and Bir-A biotin ligase pcDNA-3.1 plasmids into 1 mL of DMEM. Add 60 μL of Turbofect™ to this solution, mix via inversion, and incubate at room temperature for 15 min.
4. Add the transfection solution dropwise and incubate cells for 72 h in a 37 °C, 5% CO_2 incubator (*see* **Note 18**).
5. Harvest the medium from the cells and adjust to 50 mL (per 30 mm dish) using Ni-NTA wash buffer. Let stand on ice for 5 min.
6. Centrifuge the harvested medium at 300 × *g* for 20 min at 4 °C. Collect the supernatant and adjust to 300 mL (per 30 cm dish) using Ni-NTA wash buffer.
7. Add 300 μL (per 30 cm dish) of Ni-NTA resin (suspended in wash buffer) to the harvested medium and incubate at 4 °C with gentle stirring overnight.
8. In a cold room or large refrigerator, load the solution into a reusable nickel chromatography column. Let stand for 5 min to allow the Ni-NTA resin to settle. Purify using 2 column volumes of wash buffer (discard) followed by 1/10 column volumes of elution buffer.
9. Load eluate onto a 10kD centrifugal concentrator and centrifuge at 300 × *g* for 20 min at 4 °C, discarding the flow through. Aliquot the reserved solution and store at −80 °C.

3.6 Tracking and Analysis of Neurotrophin Axonal Transport

The brightness of quantum dots allows visualization of single particle neurotrophin transport without the need for expensive confocal microscopy. However, confocal microscopy is recommended for maximum visual fidelity. Biotinylated BDNF and proNGF are both easily conjugated to streptavidin-conjugated quantum dots. However, the conditions required to promote the transport of BDNF and proNGF are different and are discussed below.

3.6.1 Conjugation of Quantum Dots and Administration of Labeled BDNF to Axon Terminals

1. 24 h prior to the transport assay, view the neurons under a widefield microscope using bright-field light to confirm that the axonal compartment is populated with axonal projections. If axons are present, replace the axonal medium with neurotrophin-free axonal imaging medium. Incubate the neurons for 24 h at 37 °C, 5% CO_2. BFCN axons usually populate the axonal compartment by days in vitro (DIV) 5–7.
2. In a biosafety cabinet, add 1 μL of Qdot625 streptavidin conjugate stock solution to 20 μL of 300 nM biotinylated BDNF solution. Mix via brief centrifugation, and incubate on ice, protected from light, for 1 h (*see* **Note 19**).
3. Dilute the QD-BDNF solution to 1 nM using axonal imaging medium.

4. (Optional) Dilute TubulinTracker™ Deep Red 1:1000 into both the somal and axonal imaging medium.
5. Administer 80 μL of the dilute QD-BDNF solution to the top right well, wait 30 s, and repeat with the bottom right well (*see* **Note 20**). Incubate for 1 h at 37 °C, 5% CO_2. During this time, equilibrate the microscope stage to 37 °C, 5% CO_2 (*see* **Note 21**).
6. Wash the axonal side 3 times with 120 μL of axonal imaging medium before imaging.

3.6.2 Conjugation of Quantum Dots and Administration of Labeled proNGF to Axon Terminals

1. Observe neurons under a widefield microscope using bright-field light to confirm that the axonal compartment is populated with axonal projections. Return the chambers to the incubator.
2. In a biosafety cabinet, add 1 μL of QD625 streptavidin conjugate stock solution to 20 μL of 400pM biotinylated proNGF solution. Mix via brief centrifugation, and incubate on ice, protected from light, for 1 h (*see* **Note 19**).
3. Dilute the QD-proNGF solution to a final concentration of 50pM using axonal imaging medium.
4. (Optional) Dilute TubulinTracker™ Deep Red 1:1000 into both the somal and axonal imaging medium.
5. Aspirate the medium from all wells and replace the medium in the top left well with 150 μL of somal imaging medium. Immediately replace the medium in the top left well with 80 μL of the dilute QD-proNGF solution. Repeat for the bottom two wells (*see* **Note 22**).
6. Incubate for at least 15 min at 37 °C, 5% CO_2. During this time, equilibrate the microscope stage to 37 °C, 5% CO_2 (*see* **Note 22**).

3.6.3 Image Acquisition

1. Stage neurons in either a widefield or confocal microscope equipped with an on-stage incubator, 60–100× oil immersion objective (N.A 1.40), and requisite fluorescent filter cubes (*see* **Notes 5** and **6**).
2. Focus on the neurons using bright-field light. Translate the stage toward the middle of the device so that the microgrooves are visible.
3. Switch to either the Qdot625 or Texas Red channels and search for labeled neurotrophins traversing the microgrooves (*see* **Note 23**). Quantum dots exhibit a blinking behavior and are very sensitive to focus changes, making them difficult to locate at first.
4. Once the labeled neurotrophins have been located, create a time lapse by acquiring images at a single location at fixed intervals. Our lab uses intervals of 2–5 s for time lapses lasting

2–5 min. If TubulinTracker™ is being used, acquire a single image of the axon projections at the desired site using the Cy5 channel before beginning the time-lapse (*see* **Note 24**).

5. Repeat **step 4** on as many QD-positive microgrooves as possible. A minimum of 5 microgrooves containing at least 20 QD particles in total is recommended for statistical analysis. When using a 60× objective, microgrooves can be divided into approximately 3 nonoverlapping sections: retrograde (proximal to the axonal channel), middle, and anterograde (proximal to the somal channel). Ensure time-lapses are taken at all locations (*see* **Note 25**). Distal projections within the axonal compartment can also be imaged for the purposes of determining axonal uptake (*see* **Note 26**).

3.6.4 Image Analysis

1. Import time-lapse images into ImageJ by selecting "File > Import > Image Sequence…" and selecting the first image within the sequence, ensuring that all the images from the time-lapse are within a single folder and are in chronological order based on file name.
2. Open the "Properties" window by pressing "Control + Shift + P" and ensure that the "Pixel width" unit is in μM and not inches. If inches are selected by default, simply type "um" in its place. Set the "Frame interval" to the time interval between each of the images within the time-lapse.
3. Select "MTrackJ" under the "Plugins" tab of the ImageJ toolbar. The efficiency of retrograde transport can be determined in multiple ways using this plugin, the simplest of which compares how many particles are present in the section of the microgrooves closest to the cell body compartment between conditions. To do this, select "Tracking" on the MTrackJ pop-up menu and uncheck the "move to next time index after adding point" option. Individual particles can then be indexed by simply pressing "add" on the MTrackJ menu and clicking on the dots. This can be done using the "Multi point tool" (without MTrackJ, present on the ImageJ toolbar by default) if there are a small number of dots present.
4. Retrograde transport can also be assessed by quantifying the speed and pause duration of individual neurotrophin particles using MTrackJ. To do this, select "Tracking" on the MTrackJ pop-up menu and check the "move to next time index after adding point" option. Select "Add" on the MTrackJ popup menu and continually click on the particle to trace its path (*see* **Note 27**). Repeat this process with all visible particles in the time-lapse and select "Measure" on the MTrackJ popup menu. Particle speed can be calculated by taking the average value of the "v (μm/s)" column per particle. Pause duration can be

calculated by multiplying the number of instances where the speed of a particle is 0 μm/s by the frame duration of the time-lapse. Approximately 60–100 particles per group are recommended for statistical analysis.

5. Finally, retrograde transport can also be assessed by generating kymographs from the time-lapse images to trace the overall path of the particles. To do this, first repeat **step 2** and then draw a single, straight line across a single microgroove using the "Single segmented line tool" found on the ImageJ toolbar. Open the KymoToolBox plugin by navigating to "Plugins > KymoToolBox> Draw Kymo" from the ImageJ menu bar and set the width value to 100. Particle speed can also be calculated from kymographs by calculating the slope of the path traced by the particles. However, we recommend determining particle speed using single particle analysis via MTrackJ. The clarity of the kymograph can be improved by pressing "Control + Shift + C" and adjusting the brightness and contrast sliders. If images were saved as greyscale, we recommend inverting the lookup table (LUT) for better clarity by pressing the "LUT" button on the ImageJ toolbar and selecting "Invert LUT."

4 Notes

1. Each of the 4 wells of the microfluidic chamber holds only ~150 μL of media. Because of this small volume, significant evaporation occurs during handling. We recommend that chambers be handled in humidity-controlled containers (Proprietary ChipTrays™ from Xona Microfluidics, or any suitable holder with a small water reservoir) and in an incubator that is seldom opened, if possible, to avoid any confounding effects linked to excess evaporation.
2. Ensure that the opening of the pipette is not bent or sealed during the fire polishing process. An opening of <1 mm will result in reduced cell yield due to excessive shearing force during trituration.
3. We do not recommend using maintenance medium older than 1 week to ensure the health of BFCNs in culture. Preparing multiple aliquots of medium components for the quick and convenient preparation of small volumes of maintenance medium is recommended.
4. XC450 devices are made of an optically neutral plastic that is not compatible with most mineral-based immersion oils.
5. While quantum-dot streptavidin conjugates are available in a variety of wavelengths, we do not recommend the use of conjugates in the yellow-green spectrum due to their relatively

weak fluorescence compared to conjugates in the orange-red spectrum. We recommend the 625 variant, as its emission spectrum aligns very well with the commonly used Texas Red filter set.

6. Quantum dots exhibit a very large stokes shift in their excitation–emission properties. Qdot filter cube sets account for this shift and are recommended for optimal imaging. However, the brightness of quantum dots allows nonproprietary filter cube sets to be used, albeit with higher background noise due to the increased light intensities required to excite quantum dots using nonoptimal wavelengths.
7. The fluorescent labeling of tubulin using TubulinTracker™ in live cells is helpful, but not required, for imaging axonal projections within microgrooves (standard brightfield microscopy can also be used to image axonal projections, but with less clarity). While our lab has not observed significant differences in neurotrophin uptake and transport between labeled and unlabeled conditions, we recommend running pilot experiments using both labeled and unlabeled neurons to ensure that the labeling does not interfere with axonal transport in your specific experimental paradigm.
8. It is *critical* to adhere to the listed standing times during microfluidic chamber preparation. These standing times allow liquid to fully penetrate throughout all compartments of the device, reducing the risk of air bubble formation within the main channels. Refer to Fig. 6 for an example of an improperly prepared chamber containing an air bubble.
9. It is *critical* to never completely aspirate liquid from the wells of the devices. A residual volume of approximately 20 μL remaining within each well is recommended to avoid forming air bubbles and drying out the cells in the main channel.
10. Solutions should be aspirated from the top 2 wells of all devices first, followed by the bottom 2 (Fig. 2). This creates a transient volume difference across the top and bottom of the device, ensuring adequate liquid flow within the main channel.
11. Air bubbles within the main channel must be removed before plating cells. This can be done by placing the tip of a micropipette against the opening of the main channel and gently depressing and releasing the plunger.
12. Our protocol is compatible with both rat and mouse embryonic tissue. Please be sure to follow all institutional guidelines regarding proper animal care and safety during the euthanasia and dissection process.
13. A helpful video of this procedure is included in Schnitzler et al. 2008 [53].

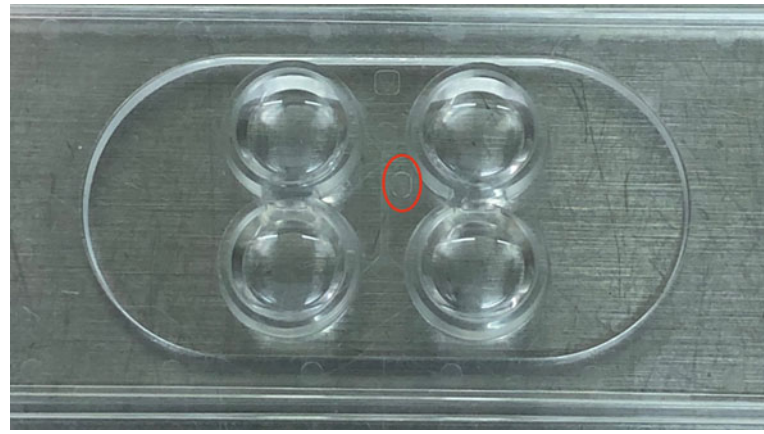

Fig. 6 A microfluidic device with an air bubble (marked with a red oval) present within one of the 2 main channels

14. The tissue from three Sprague-Dawley rat embryos is usually sufficient to prepare 8 microfluidic chambers.
15. The devices are symmetrical, and any side can be used to house the cell bodies.
16. The axonal transport of BDNF and proNGF is reduced in BFCNs after 18 days in vitro [10].
17. XC450 devices are designed to fit into most standard slide holders.
18. HEK293 cells should be plated in petri dishes as opposed to flasks to facilitate the dropwise addition of the transfection solution.
19. The neurotrophin concentration can be increased or decreased depending on the experimental paradigm. However, the ratio of neurotrophin to quantum dots should remain constant.
20. Maintaining an 80 μL volume difference between the somal and axonal sides of the chambers creates a small anterograde liquid flux, ensuring that any retrograde transport is due to axonal uptake and not incidental retrograde liquid flux.
21. BDNF uptake is significantly more rapid in BFCNs compared to cortical neurons [10]. If cortical neurons are being used, incubate the QD-BDNF solution for 4 h before imaging.
22. proNGF uptake is significantly more efficient compared to BDNF uptake in BFCNs and can be visualized using concentrations within the picomolar range [10]. The uptake also occurs much more rapidly, with QD-proNGF particles appearing in axons within 15 min [10]. Unlike BDNF, proNGF uptake is significantly inhibited upon axonal neurotrophin starvation [10].

23. Excessive exposure of neurons to light from the QD625 filter cube set is damaging due to its use of high-energy 445 nm light to maximally excite the quantum dots. We recommend minimizing both the light intensity and duration neurons are exposed to this light to avoid damaging cells.
24. We recommend staggering the incubation of individual chambers with labeled neurotrophins by between 30 min to 1 h to account for the time it takes to image a single chamber.
25. Ensure that time-lapses at each of the three sections of the microgrooves are taken at identical time intervals after neurotrophin addition to avoid the passage of time as a confound when comparing chambers.
26. Time-lapses are not necessary when imaging axonal projections for the purposes of assessing neurotrophin uptake. Uptake can simply be quantified by counting labeled particles present within a predefined length of distal axon (our lab uses 100 μm). Length can be measured using the "Straight segmented line tool" in ImageJ.
27. Neurotrophin particles can exhibit bidirectional movement during transport within the span of a single time lapse. It is recommended to analyze the retrograde and anterograde components of a given particle's transport separately. This can be done by selecting "Add" in the MTrackJ popup window following the completion of the retrograde movement of a particle and treating the anterograde component of its movement as a separate particle.

Acknowledgments

We thank Dr. Chengbiao Wu (Department of Neurosciences, University of California at San Diego, La Jolla, CA, USA) for providing us with an NGF-Avi-His plasmid and for his assistance in the development of our monobiotinylated neurotrophin purification protocols. Supported by grant #PJT-159493 from the Canadian Institutes of Health Research to MF.

References

1. Terenzio M, Schiavo G, Fainzilber M (2017) Compartmentalized signaling in neurons: from cell biology to neuroscience. Neuron 96:667–679. https://doi.org/10.1016/j.neuron.2017.10.015
2. Maday S, Twelvetrees AE, Moughamian AJ, Holzbaur ELF (2014) Axonal transport: cargo-specific mechanisms of motility and regulation. Neuron 84:292–309. https://doi.org/10.1016/j.neuron.2014.10.019
3. Rao AN, Baas PW (2018) Polarity sorting of microtubules in the axon. Trends Neurosci 41:77–88. https://doi.org/10.1016/j.tins.2017.11.002
4. Roberts AJ, Kon T, Knight PJ et al (2013) Functions and mechanics of dynein motor

proteins. Nat Rev Mol Cell Biol 14:713–726. https://doi.org/10.1038/nrm3667
5. Hirokawa N (1998) Kinesin and dynein superfamily proteins and the mechanism of organelle transport. Science 279:519–526. https://doi.org/10.1126/science.279.5350.519
6. van Spronsen M, Mikhaylova M, Lipka J et al (2013) TRAK/Milton motor-adaptor proteins steer mitochondrial trafficking to axons and dendrites. Neuron 77:485–502. https://doi.org/10.1016/j.neuron.2012.11.027
7. Lin MY, Sheng ZH (2015) Regulation of mitochondrial transport in neurons. Exp Cell Res 334:35–44
8. Debattisti V, Gerencser AA, Saotome M et al (2017) ROS control mitochondrial motility through p38 and the motor adaptor Miro/Trak. Cell Rep 21:1667–1680. https://doi.org/10.1016/j.celrep.2017.10.060
9. Moughamian AJ, Osborn GE, Lazarus JE et al (2013) Ordered recruitment of dynactin to the microtubule plus-end is required for efficient initiation of retrograde axonal transport. J Neurosci 33:13190–13203. https://doi.org/10.1523/JNEUROSCI.0935-13.2013
10. Shekari A, Fahnestock M (2019) Retrograde axonal transport of BDNF and proNGF diminishes with age in basal forebrain cholinergic neurons. Neurobiol Aging 84:131–140. https://doi.org/10.1016/j.neurobiolaging.2019.07.018
11. Fahnestock M, Shekari A (2019) ProNGF and neurodegeneration in Alzheimer's disease. Front Neurosci 13:129. https://doi.org/10.3389/fnins.2019.00129
12. Woolf NJ (1991) Cholinergic systems in mammalian brain and spinal cord. Prog Neurobiol 37:475–524. https://doi.org/10.1016/0301-0082(91)90006-m
13. Ballinger EC, Ananth M, Talmage DA, Role LW (2016) Basal forebrain cholinergic circuits and signaling in cognition and cognitive decline. Neuron 91:1199–1218. https://doi.org/10.1016/j.neuron.2016.09.006
14. Köppen JR, Stuebing SL, Sieg ML et al (2016) Cholinergic deafferentation of the hippocampus causes non-temporally graded retrograde amnesia in an odor discrimination task. Behav Brain Res 299:97–104. https://doi.org/10.1016/j.bbr.2015.11.021
15. Ypsilanti AR, Girão da Cruz MT, Burgess A, Aubert I (2008) The length of hippocampal cholinergic fibers is reduced in the aging brain. Neurobiol Aging 29:1666–1679. https://doi.org/10.1016/j.neurobiolaging.2007.04.001
16. Whitehouse PJ, Hedreen JC, White CL, Price DL (1983) Basal forebrain neurons in the dementia of Parkinson disease. Ann Neurol 13:243–248. https://doi.org/10.1002/ana.410130304
17. Ferreira-Vieira TH, Guimaraes IM, Silva FR, Ribeiro FM (2016) Alzheimer's disease: targeting the cholinergic system. Curr Neuropharmacol 14:101–115. https://doi.org/10.2174/1570159X13666150716165726
18. Whitehouse P, Price D, Struble R et al (1982) Alzheimer's disease and senile dementia: loss of neurons in the basal forebrain. Science 215:1237–1239. https://doi.org/10.1126/science.7058341
19. Ginsberg SD, Mufson EJ, Alldred MJ et al (2011) Upregulation of select rab GTPases in cholinergic basal forebrain neurons in mild cognitive impairment and Alzheimer's disease. J Chem Neuroanat 42:102–110. https://doi.org/10.1016/j.jchemneu.2011.05.012
20. Schmitz TW, Nathan Spreng R (2016) Basal forebrain degeneration precedes and predicts the cortical spread of Alzheimer's pathology. Nat Commun 7:13249. https://doi.org/10.1038/ncomms13249
21. Whitehouse PJ (1998) The cholinergic deficit in Alzheimer's disease. J Clin Psychiatry 59 (Suppl 1):19–22
22. Hyman B, Van Hoesen G, Damasio A, Barnes C (1984) Alzheimer's disease: cell-specific pathology isolates the hippocampal formation. Science 225:1168–1170. https://doi.org/10.1126/science.6474172
23. Baker-Nigh A, Vahedi S, Davis EG et al (2015) Neuronal amyloid-β accumulation within cholinergic basal forebrain in ageing and Alzheimer's disease. Brain 138:1722–1737. https://doi.org/10.1093/brain/awv024
24. Schmitz TW, Nathan Spreng R, Weiner MWM et al (2016) Basal forebrain degeneration precedes and predicts the cortical spread of Alzheimer's pathology. Nat Commun 7:13249. https://doi.org/10.1038/ncomms13249
25. Bothwell M (2014) NGF, BDNF, NT3, and NT4. In: Lewin G, Carter B (eds) Neurotrophic factors, Handbook of experimental pharmacology, vol 220. Springer, Berlin, pp 3–15
26. Alderson RF, Alterman AL, Barde YA, Lindsay RM (1990) Brain-derived neurotrophic factor increases survival and differentiated functions of rat septal cholinergic neurons in culture. Neuron 5:297–306. https://doi.org/10.1016/0896-6273(90)90166-d
27. Sanchez-Ortiz E, Yui D, Song D et al (2012) TrkA gene ablation in basal forebrain results in

dysfunction of the cholinergic circuitry. J Neurosci 32:4065–4079. https://doi.org/10.1523/JNEUROSCI.6314-11.2012

28. Latina V, Caioli S, Zona C et al (2017) Impaired NGF/TrkA signaling causes early AD-linked presynaptic dysfunction in cholinergic primary neurons. Front Cell Neurosci 11:68. https://doi.org/10.3389/fncel.2017.00068
29. Hartikka J, Hefti F (1988) Development of septal cholinergic neurons in culture: plating density and glial cells modulate effects of NGF on survival, fiber growth, and expression of transmitter-specific enzymes. J Neurosci 8:2967–2985
30. Hatanaka H, Tsukui H, Nihonmatsu I (1988) Developmental change in the nerve growth factor action from induction of choline acetyltransferase to promotion of cell survival in cultured basal forebrain cholinergic neurons from postnatal rats. Dev Brain Res 39:85–95. https://doi.org/10.1016/0165-3806(88)90069-7
31. Rylett RJ, Williams LR (1994) Role of neurotrophins in cholinergic-neurone function in the adult and aged CNS. Trends Neurosci 17:486–490. https://doi.org/10.1016/0166-2236(94)90138-4
32. Hefti F (1986) Nerve growth factor promotes survival of septal cholinergic neurons after fimbrial transections. J Neurosci 6:2155–2162. https://doi.org/10.1523/JNEUROSCI.06-08-02155.1986
33. Sun CB-Y, Xia Y et al (2013) Functional switch from pro-neurotrophins to mature neurotrophins. Curr Protein Pept Sci 14:617–625. https://doi.org/10.2174/1389203711209070658
34. Clewes O, Fahey MS, Tyler SJ et al (2008) Human ProNGF: biological effects and binding profiles at TrkA, P75NTRand sortilin. J Neurochem 107:1124–1135. https://doi.org/10.1111/j.1471-4159.2008.05698.x
35. Fahnestock YG, Michalski B et al (2004) The nerve growth factor precursor proNGF exhibits neurotrophic activity but is less active than mature nerve growth factor. J Neurochem 89:581–592. https://doi.org/10.1111/j.1471-4159.2004.02360.x
36. Ioannou M, Fahnestock M (2017) ProNGF, but not NGF, switches from neurotrophic to apoptotic activity in response to reductions in TrkA receptor levels. Int J Mol Sci 18:599. https://doi.org/10.3390/ijms18030599
37. Koshimizu H, Kiyosue K, Hara T et al (2009) Multiple functions of precursor BDNF to CNS neurons: negative regulation of neurite growth, spine formation and cell survival. Mol Brain 2:27. https://doi.org/10.1186/1756-6606-2-27
38. Fahnestock MB, Xu B, Coughlin M (2001) The precursor pro-nerve growth factor is the predominant form of nerve growth factor in brain and is increased in Alzheimer's disease. Mol Cell Neurosci 18:210–220. https://doi.org/10.1006/mcne.2001.1016
39. Garcia KLP, Yu G, Nicolini C et al (2012) Altered balance of proteolytic isoforms of pro-brain-derived neurotrophic factor in autism. J Neuropathol Exp Neurol 71(4):289–297. https://doi.org/10.1097/NEN.0b013e31824b27e4
40. Michalski B, Fahnestock M (2003) Pro-brain-derived neurotrophic factor is decreased in parietal cortex in Alzheimer's disease. Mol Brain Res 111:148–154. https://doi.org/10.1016/S0169-328X(03)00003-2
41. Seiler M, Schwab ME (1984) Specific retrograde transport of nerve growth factor (NGF) from neocortex to nucleus basalis in the rat. Brain Res 300:33–39. https://doi.org/10.1016/0006-8993(84)91338-6
42. Lu B, Nagappan G, Lu Y (2014) BDNF and synaptic plasticity, cognitive function, and dysfunction. In: Lewin G, Carter B (eds) Neurotrophic factors, Handbook of experimental pharmacology, vol 220. Springer, Berlin, pp 223–250
43. Lauterborn JC, Bizon JL, Tran TMD, Gall CM (1995) NGF mRNA is expressed by GABAergic but not cholinergic neurons in rat basal forebrain. J Comp Neurol 360:454–462. https://doi.org/10.1002/cne.903600307
44. Ha DH, Robertson RT, Roshanaei M, Weiss JH (1999) Enhanced survival and morphological features of basal forebrain cholinergic neurons in vitro: Role of neurotrophins and other potential cortically derived cholinergic trophic factors. J Comp Neurol 406:156–170. https://doi.org/10.1002/(SICI)1096-9861(19990405)406:2<156::AID-CNE2>3.0.CO;2-K
45. DiStefano PS, Friedman B, Radziejewski C et al (1992) The neurotrophins BDNF, NT-3, and NGF display distinct patterns of retrograde axonal transport in peripheral and central neurons. Neuron 8:983–993. https://doi.org/10.1016/0896-6273(92)90213-W
46. Scott SA, Mufson EJ, Weingartner JA et al (1995) Nerve growth factor in Alzheimer's disease: increased levels throughout the brain coupled with declines in nucleus basalis. J Neurosci 15:6213–6221. https://doi.org/10.1523/JNEUROSCI.15-09-06213.1995

47. Salehi A, Delcroix J-D, Belichenko PV et al (2006) Increased app expression in a mouse model of Down's syndrome disrupts NGF transport and causes cholinergic neuron degeneration. Neuron 51:29–42. https://doi.org/10.1016/j.neuron.2006.05.022
48. Taylor AM, Blurton-Jones M, Rhee SW et al (2005) A microfluidic culture platform for CNS axonal injury, regeneration and transport. Nat Methods 2:599–605. https://doi.org/10.1038/nmeth777
49. Taylor AM, Rhee SW, Jeon NL (2006) Microfluidic chambers for cell migration and neuroscience research. Methods Mol Biol 321:167–178
50. Sung K, Maloney MT, Yang J, Wu C (2011) A novel method for producing monobiotinylated, biologically active neurotrophic factors: an essential reagent for single molecule study of axonal transport. J Neurosci Methods 200:121–128. https://doi.org/10.1016/j.jneumeth.2011.06.020
51. Sobreviela T, Clary DO, Reichardt LF, Brandabur MM, Kordower JH, Mufson EJ. (1994) TrkA-immunoreactive profiles in the central nervous system: colocalization with neurons containing p75 nerve growth factor receptor, choline acetyltransferase, and serotonin. J Comp Neurol 350(4):587–611. https://doi.org/10.1002/cne.903500407
52. Holtzman DM, Li Y, Parada LF et al (1992) p140trk mRNA marks NGF-responsive forebrain neurons: evidence that trk gene expression is induced by NGF. Neuron 9:465–478. https://doi.org/10.1016/0896-6273(92)90184-F
53. Schnitzler AC, Lopez-Coviella I, Blusztajn JK (2008) Purification and culture of nerve growth factor receptor (p75)-expressing basal forebrain cholinergic neurons. Nat Protoc 3:34–40. https://doi.org/10.1038/nprot.2007.477